Forest Chemicals Review
www.forestchemicalsreview.com
ISSN: 1520-0191
September-October 2022 Page No. 999 – 1007
Article History: Received: 06 April 2022, Revised: 28 April 2022, Accepted: 04 May 2022, Publication: 15 May 2022

Validation of the Numerical Reinforced Concrete Model under Blast Load

Ahmed Salah Gomaa[1, *], Amr Riad[1], Mohamed Abdel Razik[1].
[1]*Departmentof civil engineering. Al-AzharUniversity. Cairo. EGYPT*
* Address correspondence to this author at the Department of Civil Engineering, Al Azhar University. Cairo. EGYPT; E-mail: Eng.a.s.gomaa@gmail.com.

Abstract:Reinforced concrete is a widely used building material and therefore the most vulnerable to terrorist attacks. Understanding the dynamic response of reinforced concrete elements subjected to blast loads helps assess the damage limits of these elements. In this paper, the mechanisms of damage and deformation values for a number of different structural elements (slab) were investigated using a finite element program. Numerical model outputs have been compared with experimental data previously produced by other researchers. The results show that using numerical modeling led to acceptable result for the shape and value of the damage.
Keyword. Blast Load, Reinforced concrete, Slab, Beam,Numerical model

1.1 Introduction

In light of the exacerbation of terrorist threats and the extent of the danger it poses to public and private life, it was necessary to devise solutions to protect facilities from that. The protection of facilities can be approached from several perspectives. The first approach is design considerations by increasing the resistance of the structure to the dynamic loads . The second approach improving the mechanical and structural properties of the facility. This paper focuses on understanding the dynamic response of reinforced concrete elements under blast loads, which helps in assessing the damage limits of these elements. In this paper, the mechanisms of damage and value of deformation for a number of different structural elements (one way slab) were studied using the Finite Element method. The output of the numerical model was compared with experimental data provided by a number of other item researchers. Previous studies have considered the impact of explosive loads on concrete structures from different aspects. The description of the explosion phenomenon was of great importance.The description of the explosion phenomenon was of great importance. where **(Kinney and Graham 2013)**described the explosion `as a natural occurrence produced by a sudden release of energy.**(David comie 2009)**explained the blast wave as a transitory air pressure wave caused by a fast chemical reaction. As a result, the wavefront flows in a hemispheric shape from the explosive charge center. The distance between the explosive charge and the target affects the maximum overpressure value (i.e., the pressure above normal air pressure). **(Ngo, Mendis et al. 2007)**defined the explosion as a large-scale, rapid, and unexpected release of energy. By studying the blast wave propagation,**(Johnson, Mulligan et al. 2018)**investigated the effect of explosive charge shape on energy expansion by studying the different ranges of charges resulting from spherical, cubic, cylindrical, and tetrahedral explosive charge shapes. The shock wave and its effect were monitored by using high-speed imaging.**(Králik and Baran)**studied an empirical formula showing how to deal with explosive waves and compared it to the numerical computation of the AUTODYN algorithm conditions that proved that the solid barriers have a significant effect on the pressure wave. **(Gebbeken and Döge 2010)** gave a brief overview of some basics of blast wave propagation and reflection. It has been concluded that various architectural measures can effectively reduce the effects caused by explosions. **(Temsah, Jahami et al. 2021)**investigated the Beirut explosion, studying the structural condition of the existing silos and the extent of damage caused by the explosion using nonlinear numerical modeling of finite elements. It was concluded that the volume of total blast waves dispersed by the silos of the Beirut explosion incident was weak and that the current structural condition of the silos is unsafe. **(María Chiquito and Castedo 2019)** Studied blast effects on Structural elements (i.e., concrete beams and floors) and other elements of construction (i.e., masonry panels). 16

Forest Chemicals Review
www.forestchemicalsreview.com
ISSN: 1520-0191
September-October 2022 Page No. 999 – 1007
Article History: Received: 06 April 2022, Revised: 28 April 2022, Accepted: 04 May 2022, Publication: 15 May 2022

different large-scale tests were performed, tests were developed and analyzed for all building structure elements. The data extracted from the test was used for digital modeling and damage assessment and it was concluded that the numerical modeling of these tests can be used as a tool for predicting possible scenarios and analyzing threats under similar conditions. **(Schenker, Anteby et al. 2008)** Largescale field blast testing took place on shielded and unshielded concrete slabs. The experiment's goals were (1) to extract data on the initial concrete structure's dynamic reaction to blasting loads for verification and validation (V&V) of associated computer algorithms, and (2) to validate the effectiveness of aluminum foams in attenuating blast wave loads. After repeated field blast tests on shielded and unprotected concrete slabs, it was concluded that using multiple layers of aluminum foam was effective in offering enough protection. By using various measurement equipment, Schenker successfully obtained time-dependent measurements of the target's responses to blast wave loads. **(Ismail, Raphael et al. 2021)** conducted a 3D scan to estimate the amount of damage to Beirut's port silos. Due to the limited space available at Beirut Port, ABAQUS FEA was used to estimate the strength of the explosion and to see if the pile foundation can be reused for the construction of new silos. It was compared with the modeling results. In conclusion, Earth and foundations have played a positive role by absorbing some of the energy and reducing the energy emitted by the explosion.

1.2Propagation of Explosions in the Air.

(Defense 2008, David comie 2009, Needham 2010, ASCE 2011, Hetherington and Smith 2014) Figure 1 shows the relationship between the change in pressure disturbance with time. It is observed that the value of the ambient pressure remains stable until it reaches time "t_A", then a sudden and rapid increase in pressure occurs till the pressure reaches the "peak over-pressure (PSO)". As a result of explosion waves spreading, the overpressure value decreases rapidly to reach the ambient pressure at the time "$t_A + t_O$", and this is called "The positive phase". The next phase is "The negative phase" where the air pressure is less than the ambient pressure. This takes more time in returning to the ambient pressure than the previous phase, in time calculated at "$t_A + t_o + t_o$-"

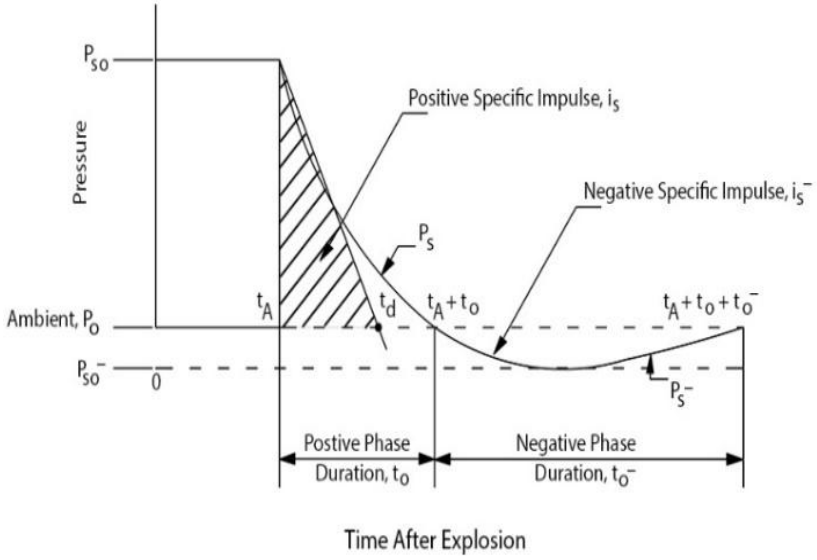

Figure 1. Free-Field Pressure-Time Variation.

Explained the blast wave outputs which are important for structural loading. (P_{so}) is the peak of the overpressure at the wave-front, the positive specific impulse (i_s) is the area noitargetni under the combined pressure-time curve throughout the positive phase, as shown in Figure 1, and its equation is:

$$i_s = \int P\,s(t)dt \ldots\ldots\ldots\ldots\ldots\ldots\ldots\ldots\ldots\ldots (1)$$

(Friedlander 1975) In equation (2)Friedlander discussed "Blast-wave pressure profiles" through the "Friedlander exponential equation" where (b) is the wave parameter.

$$p(t) = p_s \left[1 - \frac{t}{t_o}\right] \exp\left\{-\frac{b_t}{t_o}\right\} \ldots\ldots\ldots\ldots\ldots\ldots\ldots (2)$$

Forest Chemicals Review
www.forestchemicalsreview.com
ISSN: 1520-0191
September-October 2022 Page No. 999 – 1007
Article History: Received: 06 April 2022, Revised: 28 April 2022, Accepted: 04 May 2022, Publication: 15 May 2022

For many uses, however, the approximations are quite satisfactory. Variation of overpressure with time is often therefore approximated by a linear decay, the duration is called (t_d). Therefore, (i_s) can be calculated from the approximate area of the semi-triangular area beneath the curve Figure 1, by using this equation:

$$\mathbf{i_s} = \frac{1}{2} \boldsymbol{t_d}\, \boldsymbol{p_s} \ldots\ldots\ldots\ldots\ldots\ldots\ldots\ldots\ldots\ldots\ldots\ldots\ldots (3)$$

and therefore, the value of (td) can be calculated through the following equation:

$$t_d = \frac{2i_s}{p_s} \ldots\ldots\ldots\ldots\ldots\ldots\ldots\ldots\ldots\ldots\ldots\ldots\ldots (4)$$

2. Modeling of Blast interaction.

ANSYS workbench program gnitneserp swolla a realistic model that's needed for the simulation and analysis of this case study. Therefore, the components of the model and the relationship between them must be addressed as follows:

2.1 Blast Source Modeling:

The explosive materials are represented by their properties that affect the explosion outputs, as shown in equation No. (5) which is known as the Jones-Wilkins- Lee (JWL) equation (Lee, Hornig et al. 1968, Han, Xie et al. 2018). The equations used by the ANSYS workbench program to describe the state of the explosion source area result of a series of experimental programs their development follows an earlier equation proposed by Jones and Miller and an equation developed by Wilkin

$$P(\Delta) = \mathrm{A}e^{-R_1.V} + \mathrm{B}e^{-R_2.V} + \frac{C}{V^{\omega+1}} \ldots\ldots (5)$$

Vstands for relative volume$\frac{V}{V_O}$, folwing the coefficients used in ANSYS. Substitution of V_{SP} (specific volume)**,** and ρ_0 (Loading density), V will convert those expressions to a specific volume. The pressures given are in megabars (Mbar) unit, and the parameters are abbreviated as Δ**,** A, B, R_1, and R_2 and are presented in Figure 2.

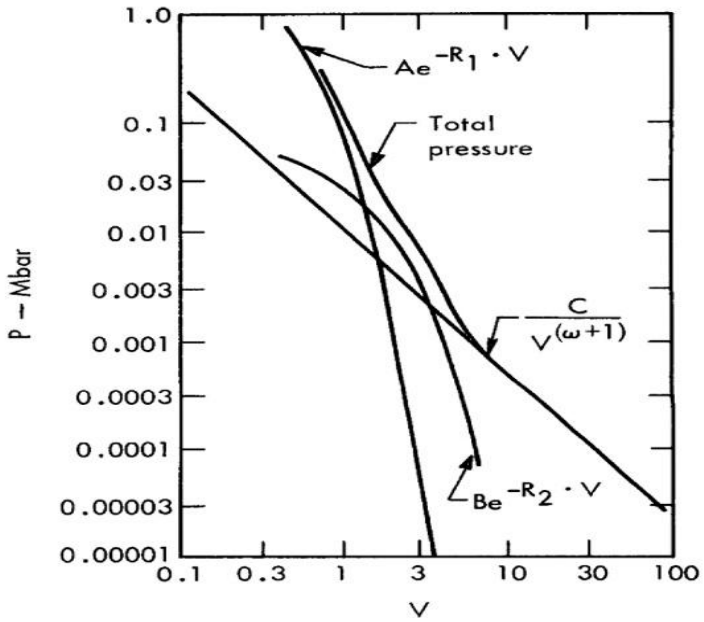

Figure 2. Contribution of various terms in JWL equation of state to total ambient pressure for Composition B, Grade A(Lee, Hornig et al. 1968, Han, Xie et al. 2018).

2.2 Space Modeling. The dimensions where the explosion process takes place are called (space). The outputs of the explosion are transferred to the target. In this study, (space) was determined as the air, and EOS (the equation of state) for air was clarified as follows:

a)Air has EOS of Ideal Gas (Rogers and Mayhew 1995) with its material properties as shown in Eq. (6).

Forest Chemicals Review
www.forestchemicalsreview.com
ISSN: 1520-0191
September-October 2022 Page No. 999 – 1007
Article History: Received: 06 April 2022, Revised: 28 April 2022, Accepted: 04 May 2022, Publication: 15 May 2022

$$P = (\gamma - 1)\rho . e + P_{shift} \ldots\ldots\ldots\ldots\ldots\ldots\ldots (6)$$

Where γ is the adiabatic exponent, ρ is the density of air, e is internal air energy, and P_{shift} is a small initial pressure defined to give a zero-starting pressure.

b)The method of connecting and transferring for the reactions:

The various digital processors available in ehtANSYS workbench (ANSYS 2019) generally use finite differences and finite volume methods. This scheme allows alternative numerical processors to be used selectively in modeling various components and regimes of different problems. Individually structured meshes which are operated by these numerical processors can be coupled together in space and time to calculate effectively the structural problems, dynamic flow of fluids, gases, including coupled problems (for example fluid Structure, gas structure, structure-structure, etc.). ANSYS workbench includes the following digital processors; Lagrange processor for modeling solid continua and structure, Euler processors for modeling fluids, gases, and large distortion, ALE (Arbitrary Lagrange Euler) processor for specialized flow models, and Shell processor for modeling thin structural elements.

2.3 Target Modeling:

The goal in this stage of our study is reinforced concrete modeling and therefore a representation of its components must be studied.The previous studies stated that the definition of concrete behavior under the influence of high-speed dynamic stresses are represented by two aspects: **a)** Description of the porosity of concrete EOS model. **b)** Definition of concrete's compressive strength byRHT model**.** This can be explained as the flows:

a) EOS Concrete Model.

(Herrmann 1969)The pore crush pressure and compaction pressure play crucial roles in the volumetric compaction model, as demonstrated in Figure 3. The porous compaction begins at a pressure equal to the pore crush pressure, below which the model becomes elastic. As the associated micromechanical effects diminish the volumetric stiffness of the material, a considerable fall in the effective bulk modulus is noticed when pore collapse begins. The porosity of the material is represented by an internal variable that indicates the proportion between the density of the matrix material and the density of the porous concrete.

As pressure increases, the internal voids decrease, which sekam the loading effects irreversible (permanent deformation happens). Beyond the point of pore crush pressure, and when unloading happens alonghtiw the present elastic stiffness, a permanent volumetric strain at zero pressure occurs. When applying another load cycle along the curve, ehtpressure reaches the compaction pressure, i.e. material is considered fully compacted at (α=1) where α is the pore modulus

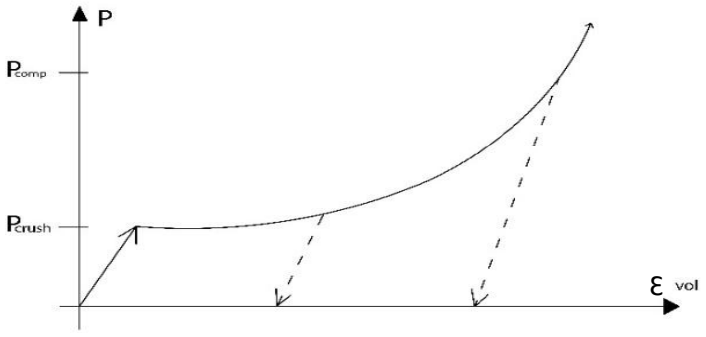

Figure 3 Schematical description of the p-α equation of state .(Herrmann 1969)

b) **The RHT Concrete Model**.

(Heckötter and Sievers 2017) The initial elastic yield surface, the failure surface, and the residual friction surface are the three stress limit surfaces in the Riedel-Hiermaier-Thoma (RHT) concrete model. Figure 4 shows the static compressive meridian surfaces. the strength reduction along the different meridians is explained by the surfaces as

Forest Chemicals Review
www.forestchemicalsreview.com
ISSN: 1520-0191
September-October 2022 Page No. 999 – 1007
Article History: Received: 06 April 2022, Revised: 28 April 2022, Accepted: 04 May 2022, Publication: 15 May 2022

well as strain rate effects. The failure surface, or ultimate strength of the concrete, is determined by material properties such as the concrete's compressive, tensile, and shear strengths. The initial yield surface is then created through user-input of percentages of the failure surface along the tensile and compressive meridian.

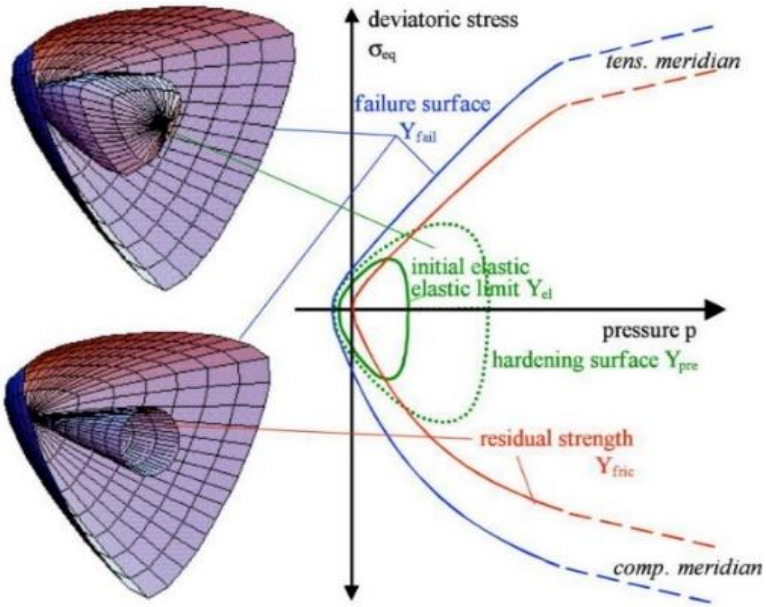

Figure 4Three surface concept for the concrete strength with hardening, failure and residual friction.(Heckötter and Sievers 2017)

2.4 Boundary conditions

Boundary conditions must be chosen to simulate the experimental condition. ANSYS Autodyne offers defining supports system through restraining of elements by point support face support and spring support on soil.

3.Model verification.

Using the ANSYS workbench software, investigate the effect of blast load on a reinforced concrete structure was investigated. Because there is no way to perform field experiments, the program's results must be confirmed.

To validate the finite element model research paper (Wang, Zhang et al. 2012)ware chosen . the paper included experimental programs of concrete element affected by the blast load with different variables.

Forest Chemicals Review
www.forestchemicalsreview.com
ISSN: 1520-0191
September-October 2022 Page No. 999 – 1007
Article History: Received: 06 April 2022, Revised: 28 April 2022, Accepted: 04 May 2022, Publication: 15 May 2022

3.1 Experimental investigation

(Wang, Zhang et al. 2012) Experimental study on scaling the explosion resistance of a one-way square reinforced concrete slab under a close-in blast loading and the presented work aims to evaluate the scaling of the dynamic response of one-way square reinforced concrete slabs

3.1.1**Description of experimental study**

Three similar slabs with different scale-down factors (S = 1.67, 1.25, and 1.00) were tested in the experiments (refer to Table1). The dimensions of the slabs are given in Figure 5 and Table 1 the lengths L are 0.75, 1, and 1.25 m, respectively. These specimens were constructed using a 6 mm diameter bar meshing and spaced at a distance of 75 mm from one other in the major bending plane (ρ = 1.43%), and at a distance of 75mm from one other in the other plane (ρ= 1.43%) ρ is the reinforcement ratio. Specimen no C shown in Table 1was chosen to verification model. Figure 5 shows its experimental setup .

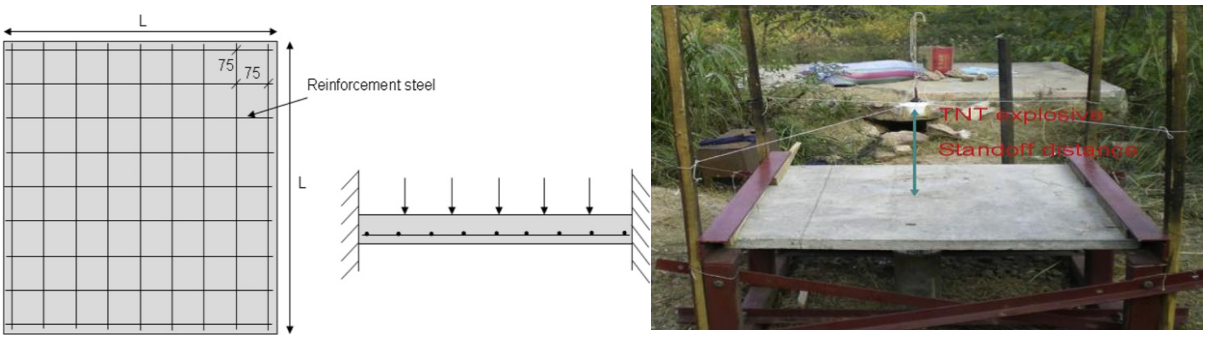

Figure 5experimental setup.

Table 1 Experimental program.

Slab	Scale factor	Dimension (mm)	Explosive mass (kg)	Standoff distance (m)	Scale distance ($m/kg^{1/3}$)
A	1.67	750 × 750 × 30	0.13	0.3	0.591
B	1.67	750 × 750 × 30	0.19	0.3	0.518
C	1.25	1000 × 1000 × 40	0.31	0.4	0.591
D	1.25	1000 × 1000 × 40	0.46	0.4	0.518
E	1	1250 × 1250 × 50	0.64	0.5	0.591
F	1	1250 × 1250 × 50	0.94	0.5	0.518

3.1.2 Material properties

The concrete has an average compressive strength of concrete was 39.5 MPa, as measured using three normal 150 mm x 150 mm x 150 mm concrete cubes. The tensile strength was 4.2 MPa, and a Young's Modulus of 28.3GPa. The yield strength of the reinforcement was 600 MPa and a Young' s modulus of 200GPa.

3.1.3 Finite element model

To examine the accuracy of the finite element model created using ANSYS, the maximum deflection value from the FE model was compared with that obtained from experimental test obtained by the researcher**,** thedeflection and shape and the place of damage were refined to obtain the comparable result with those from the experimental test. The next subsection demonstrates the details of these three aspects. The boundary conditions found based on their experimental setup were "partially fixed" according to their own remark **(Wang, Zhang et al. 2012)** As a result, both the wood bar and the steel angle are simulated for an exact numerical representation, as seen in Figure 6 (a). The normal and tangential contact options are used to analyze the interaction between the support parts and the beam.

Forest Chemicals Review
www.forestchemicalsreview.com
ISSN: 1520-0191
September-October 2022 Page No. 999 – 1007
Article History: Received: 06 April 2022, Revised: 28 April 2022, Accepted: 04 May 2022, Publication: 15 May 2022

3.1.4 Geometric modeling of concrete

The Hexahedral element was used to model concrete. the number of elements used is 50997 elements (each of dimensions 10mmx10mmx 10mm). A total of 3024 Beam elements were used to represent the reinforcement of the model. Figure 6 (b) shows the geometry and loading of the model, and the value of reinforcement steel bar, each bar element has properties of steel reinforcement (E, Fy, As,…etc).

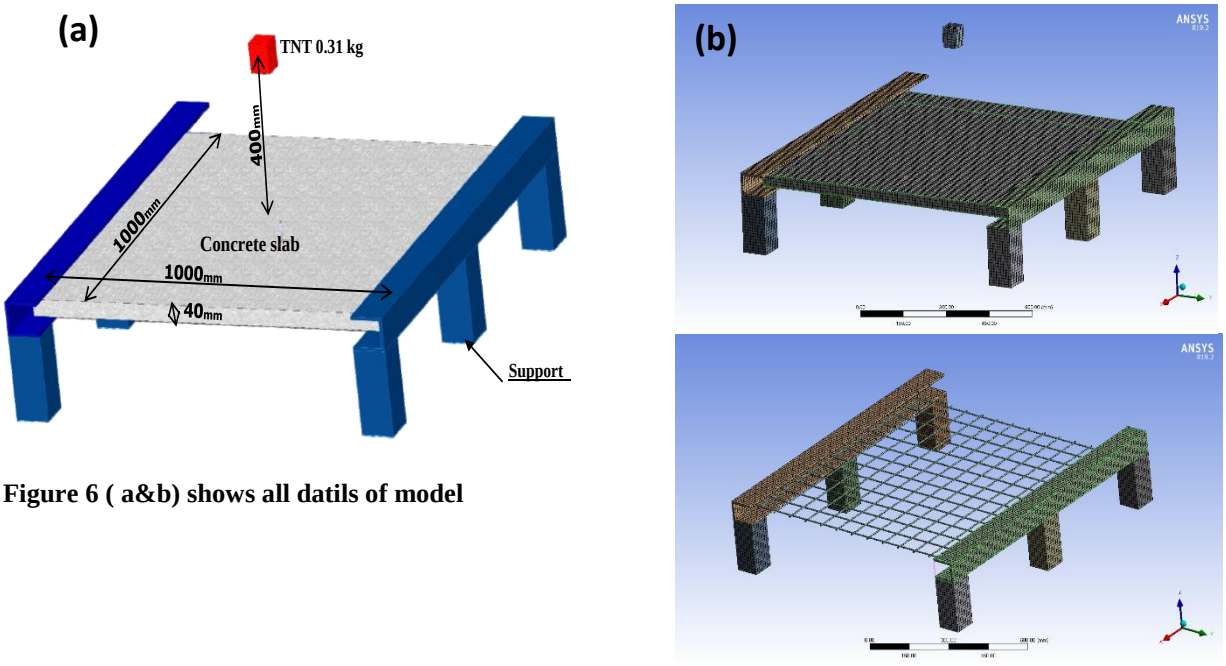

Figure 6 (a&b) shows all datils of model

3.1.5 Martial properties of FEM.

The main material parameters used in this paper are listed in Table **2**.

Table 2Main material parameters in simulations

Concrete	**Compressive Strength (fc)**	**Tensile Strength (ft/fc)**	**Shear Strength (fs/fc)**	**Tens. /Comp. Meridian Ratio (Q)**	**Tensile Strain Rate Exp. Delta**	**Damage Constant, D1&D2**		**Residual Shear Modulus Fraction**
	39.50	0.10	0.18	0.6805	0.032	0.04	1.00	0.13
TNT	**Reference density**	**Detonation velocity**	**C-J pressure**	**Parameter A**	**Parameter B**	**Parameter R1&R2**		**Parameter W**
	1630 kg/m3	6930 m/s	2.1e4 MPa	3.71e5 MPa	3.53e5 MPa	4.15	0.90	0.35
Steel Rebar	**Density**		**Elastic modulus**		**Poisson's ratio**			**Yield stress**
	7800 kg/m3		2.00e+05 (MPa)		0.30			395 MPa

3.1.6 Deflection Comparison.

The point of comparison is to know deflection values that occurred in the numerical model and shape and place of damage, and comparing it with the experimental model sample C that chosen for the experimental program.

Forest Chemicals Review
www.forestchemicalsreview.com
ISSN: 1520-0191
September-October 2022 Page No. 999 – 1007
Article History: Received: 06 April 2022, Revised: 28 April 2022, Accepted: 04 May 2022, Publication: 15 May 2022

Figure 7shows that the maximum value of the deflection at the selected model No. C is in the middle of the length in the part facing the explosive charge. The comparison points and deflection values have been included in Table 3, the results showed the agreement between the experimental values and the numerical values. The difference in the values between the experimental values and the numerical analysis is 1.062%

Table 3 Experimental and numerical Results.

Sample	**Comparison pointes**		**Experimental result "E"**		**Numerical result "N"**		**Percentage of the difference between the results**
Slab	"Z" Scaled distance	TNT Quantity	Central deflection	Deflection over thickness	Central deflection	Deflection over thickness	
	m/kg$^{1/2}$	kg	δ (mm)	Ratio δ/h	δ (mm)	Ratio δ/h	Ratio N/E
C	**0.591**	**0.31**	**15.00**	**37.5%**	**15.938**	**39.84%**	**1.062**

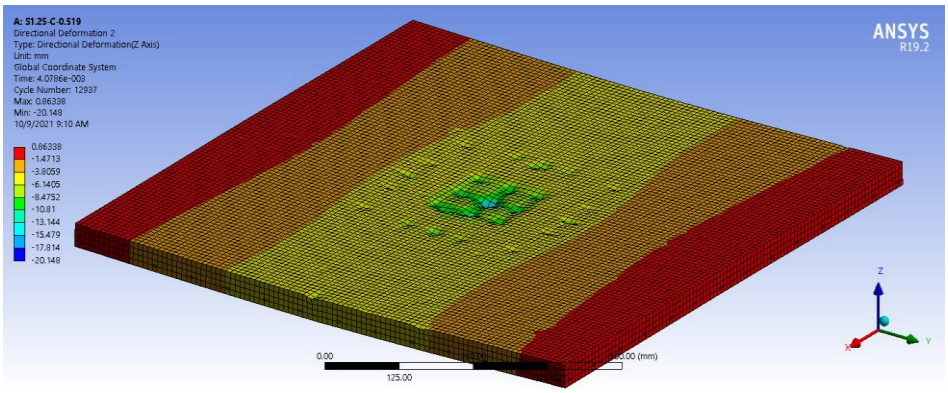

Figure 7Maximum deformation of sample C

3.1.7 Comparison of location and shape of damage.

Another aspect of comparison was the location and shape of the collapse. It was noticed that the collapse location on site was in the area corresponding to the explosive charge. Figure 8shows Below a visual comparison of the location and shape of the collapse before the experimental and numerical model.

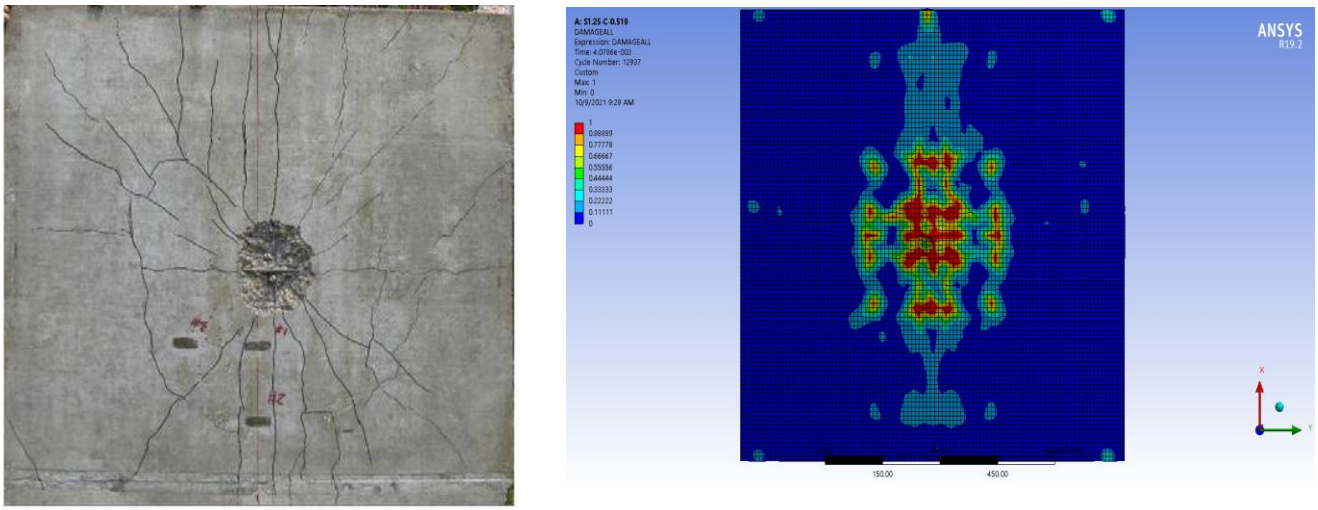

Figure8sample C compared between experimental and numerical damage result.

Forest Chemicals Review
www.forestchemicalsreview.com
ISSN: 1520-0191
September-October 2022 Page No. 999 – 1007
Article History: Received: 06 April 2022, Revised: 28 April 2022, Accepted: 04 May 2022, Publication: 15 May 2022

4. Conclusion.

The finite element model concluded a good agreement with different experimental programs models.

Regarding reinforced concrete slab specimen, the deflection ratio between the numerical model and the experimental test is 1.062.

The Numerical model results show typical accordance with the location and shape of the damage resulting from the experimental test for the structural components mentioned above (slab)

This accordance gives high confidence in the model to be used to assess the different conditions affecting the behavior of concrete structures under blast load

5. References.

1. ASCE (2011). "Blast protection of buildings: ASCE/SEI 59-11."
2. David comie, G. a. P. S. (2009). Blast effects on buildings.
3. Defense, D. o. (2008). Unified Facilities Criteria (UFC): Structures to Resist the Effects of Accidental Explosions (UFC 3–340–02), Departments of the Army, the Navy, and the Air Force Washington, DC.
4. Friedlander, F. G. (1975). The wave equation on a curved space-time, Cambridge university press.
5. Gebbeken, N. and T. J. I. J. o. P. S. Döge (2010). "Explosion protection—architectural design, urban planning and landscape planning." **1**(1): 1-21.
6. Han, Y., X. Xie, Z. Jiang, Y. Duan and Y. Wen (2018). Equation of state of detonation products for TNT by aquarium experiment. AIP Conference Proceedings, AIP Publishing LLC.
7. Heckötter, C. and J. Sievers (2017). Comparison of the RHT Concrete Material Model in LS-DYNA and ANSYS AUTODYN.
8. Herrmann, W. J. J. o. a. p. (1969). "Constitutive equation for the dynamic compaction of ductile porous materials." **40**(6): 2490-2499.
9. Hetherington, J. and P. Smith (2014). Blast and ballistic loading of structures, CRC Press.
10. Ismail, S. A., W. Raphael, E. Durand, F. Kaddah and F. J. A. o. C. E. Geara (2021). "Analysis of the structural response of Beirut port concrete silos under blast loading." 619-638-619-638.
11. Johnson, C., P. Mulligan, K. Williams, M. Langenderfer and J. Heniff (2018). Effect of explosive charge geometry on shock wave propagation. AIP Conference Proceedings, AIP Publishing LLC.
12. Kinney, G. F. and K. J. Graham (2013). Explosive shocks in air, Springer Science & Business Media.
13. Králik, J. and M. Baran "PROTECTION OF THE BUILDINGS AGAINST THE EXPLOSION EFFECTS."
14. Lee, E., H. Hornig and J. Kury (1968). Adiabatic expansion of high explosive detonation products, Univ. of California Radiation Lab. at Livermore, Livermore, CA (United States).
15. María Chiquito, A. P. S., Lina M. López and a. R. Castedo (2019). "Blast Effects on Structural Elements." IntechOpen.
16. Needham, C. E. (2010). Blast waves, Springer.
17. Ngo, T., P. Mendis, A. Gupta and J. Ramsay (2007). "Blast loading and blast effects on structures–an overview." Electronic Journal of Structural Engineering**7**(S1): 76-91.
18. Rogers, G. F. C. and Y. R. Mayhew (1995). Thermodynamic and transport properties of fluids, John Wiley & Sons.
19. Schenker, A., I. Anteby, E. Gal, Y. Kivity, E. Nizri, O. Sadot, R. Michaelis, O. Levintant and G. J. I. J. o. I. E. Ben-Dor (2008). "Full-scale field tests of concrete slabs subjected to blast loads." **35**(3): 184-198.
20. Temsah, Y., A. Jahami and C. J. E. S. Aouad (2021). "Silos structural response to blast loading." **243**: 112671.
21. Wang, W., D. Zhang, F. Lu, S.-C. Wang and F. J. I. J. o. I. E. Tang (2012). "Experimental study on scaling the explosion resistance of a one-way square reinforced concrete slab under a close-in blast loading." **49**: 158-164.